A Global Approach to Local Approximations

Luciano da Fontoura Costa

A Global Approach to Local Approximations

Luciano da F. Costa
luciano@ifsc.usp.br

São Carlos Institute of Physics – DFCM/USP

11th Jan. 2023

Abstract

Space and shape have special importance in science and technology, as they underly an impressive range of real-world structures and phenomena. Thanks to concepts and methods from calculus, it becomes possible to approximate functions, curves, surfaces, and vector fields in terms of respective first-order (tangent) approximations obtained by using the Taylor series. By providing an effective approximation, this approach has been extensively adopted not only in theoretical studies (e.g. linear approximations of non-linear dynamics), but also in the most diverse types of applications. The present work is aimed at providing an accessible introduction to first-order approximation of several mathematical mappings and structures, with emphasis on the possibility of using these approximations as a means to define local coordinate systems that adapt effectively to the studied mathematical entity. After providing a motivation about first-order approximations respectively to single-variable functions, we proceed to parametric curves, multivariate functions, implicit functions and surfaces, as well as vector fields. Several numeric case-examples and illustrations have been provided to help the consolidation of the presented topics.

"...each human being carries a personal coordinate system, an effective first-order approximation constantly adapting to the surroundings."

Excerpt from the present work.

1 Introduction

After space, shape is probably one of the aspects of the real physical world that are closest to human intuition and experience. Time eventually comes next, though being intrinsically less palpable and objective.

For us, humans, *space* typically refers to $3D$ (the geometrical world where we live), $2D$, and $1D$ Euclidean spaces. Though we seem to be well-acquainted with *shape*, this aspect of nature is not so easy to be objectively defined, generally speaking.

One aspect of shape that seems to be a consensus among humans is that it does not change under translation, rotation, reflections, and possibly scalings (e.g. [2]). In addition, shapes distinguish themselves in terms of varying respective topological and geometric properties, such as curvature and torsion (see Figure 1), which are directly related to first-order variations of the tangent field along a curve or surface.

It goes without saying that shape plays a key role in several day to day pattern recognition tasks.

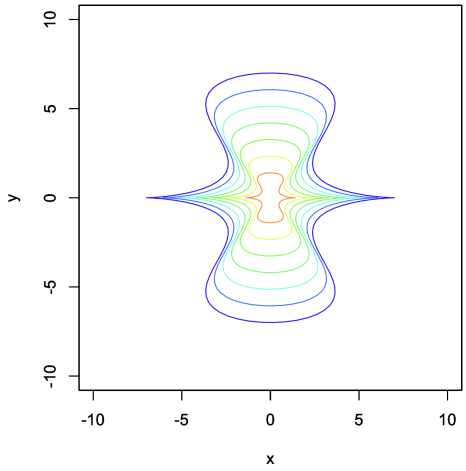

Figure 1: Space and shape are closely interrelated not only in general relativity, but in our day to day experience as well. To a great extent, the important features of shapes relate to variations of their *local* properties, such as orientation, along the embedding space. For instance, abrupt variations of the tangent field along a curve can be particularly effective in catching our attention up (saliency, e.g. [1]). In a sense, curvature can be though in analogy to a lightning rod concentrating the surrounding lines of electric field.

As a consequence of the key importance of space and shape for humans, not to mean their intrinsic relationship with nature, these two concepts underlie much of our sci-

entific and technological developments. In mathematics, too, space and shape often play a central role, not only in the more straightforward Euclidean approach, but also involving higher dimensional non-Euclidean vector spaces that can include functions and fields.

The present work is aimed at providing a reasonably accessible introduction to *local* representations of space and shape in $2D$ and $3D$ spaces, especially Euclidean cases, as well as to the local approximation of mappings, such functions and vector fields. Interestingly, *mappings* such as $y = f(x)$ can be immediately transformed into *structures*, such as the curve $(x, f(x))$ defined by the mapping.

Because such a study could easily become too broad, we focus on the key possibility to represent functions, curves, surfaces, and vector fields in terms of their respective *first-order approximations*, as allowed mainly by the *Taylor series*. In doing so, it is expected that the present work may also contribute to developing a basic background that can facilitate subsequent studies involving higher order and higher dimensional approaches possibly involving non-linear mappings.

Two main topics of theoretical and applied interest, are developed here.

First, we have the possibility to obtain effective approximations of functions, curves, surfaces, and vector fields locally, around a small neighborhood of a reference point of operation, by using the first-order respective Taylor series approximation. This principle underlies much of calculus as well as many numeric concepts and methods in a broad range of areas and applications. For instance, many non-linear dynamics can start to be investigated locally, around a respective *point of operation*.

Second, we address the possibility to establish local coordinate systems at the approximation points. The respective motivation concerns practical applications, for instance in data analysis, scientific visualization, and pattern recogntion, where one is often interested in visualizing specific portions of multidimensional data and respective representations. In a sense, it could be said that each human being carries a personal coordinate system, an effective first-order approximation constantly adapting to the surroundings.

Additional motivation for coordinate system changes have been elaborated in a previous work [3], of which the current one can indeed be considered, in many aspects, a continuation.

Despite the relative effectiveness of first-order approaches to local approximations, it should be kept in mind that, when applied to complex systems involving non-linear dynamics, a good deal of the respective structure and dynamics can be overlooked. Even so, first-order approximations remain an interesting first approach, to be possibly complemented by more comprehensive approaches.

A more effective reading of the present work will benefit from previous familiarization with basic concepts from linear algebra and multivariate calculus (e.g. [4, 5, 6, 7, 8, 9]). Two previous related works, namely [10] and [3], also complement several aspects of the current presentation respectively to trajectories as parametric curves, and basis transformations and coordinates change, respectively.

We start by presenting an overall motivation and illustration of the potential of first-order approximations respectively to single-variables functions of the type $y = f(x)$. More specifically, it is shown how non-linear functions can be locally approximated around a point of reference, and how these approximations pave the way to effective estimation for calculations (e.g. integration) around this point, as well as for defining local coordinate systems that adapt to the shape of the function. These possibilities are then discussed respectively to several other mathematical entities, namely parametric curves, multivariate functions, parametric surfaces, and vector fields. A brief discussion about the accuracy of first order approximations concludes the presentation.

2 Single Variable Motivation

To a considerable extent, the concepts of first order derivative and differential have played a systematic and decisive role in scientific and technological advancements, underlying almost every mathematics-based approach.

Though these concepts may appear somewhat abstract and intricate when applied to multivariate functions, surfaces and vector fields, it turns out that they are really simple and approachable, especially when intuitive geometrical terms are taken into account. In addition, a more thorough knowledge about the simplest situation involving single-variable functions can also substantially contribute to studies of more elaborate mappings and structures, because all these cases share to a large extent the same motivation, concepts and methods.

In this section, we aim at developing the concept of first order derivative and differential regarding this simplest case, involving single variable functions.

Provided it can be calculated, the first derivative of $g()$ at a generic point x can be expressed as:

$$\frac{d\,g(x)}{dx} = \dot{g}(x) \tag{1}$$

which allows us to approximate $g(x)$ in terms of the respective first-order Taylor series as follows:

$$\boxed{g(x)\big|_{x_0} \approx \tilde{g}(x)\big|_{x_0} = g(x_0) + \dot{g}(x_0)\,(x - x_0)}. \tag{2}$$

where we shall use the notation "$|_{x_0}$" to indicate a small neighborhood around the reference point x_0.

By introducing the abbreviation $m = \dot{g}(x_0)$, we can rewrite Equation 2 as:

$$g(x)\big|_{x_0} \approx \tilde{g}(x)\big|_{x_0} = m\,(x - x_0) + g(x_0) =$$
$$= m\,x - m\,x_0 + g(x_0) = m\,x + c$$
$$\text{where: } c = -m\,x_0 + g(x_0)$$

Though simple, this result is important enough to be boxed:

$$\boxed{g(x)\big|_{x_0} \approx m\,x + c} \tag{3}$$

Basically, we have that the Taylor series approximation around point x_0 corresponds simply to a straight line equation.

Interestingly, in a wide range of cases in which $g(x)$ is reasonably smooth around the reference point, this can be found to provide an effective approximation of the original function $g(x)$ around a small neighborhood of x around x_0.

This property is particularly important because it allows us to represent and handle (e.g. differentiate, integrate, extrapolate, change coordinates, etc.), within a given accuracy, the original function $g(x)$ in terms of a simpler representation as a line function. As a matter of fact, the first order approximation of a function as above underlies a vast range of theoretical and numerical concepts and methods in mathematics, some of them to be addressed in the present work.

Let us consider the following numeric example:

$$g(x) = 0.1\,x^3 + 0.2\,x^2 + 0.3\,x + 0.1 \tag{4}$$
$$x_0 = 1 \tag{5}$$

Fractional coefficients have been adopted in this third-degree polynomial for the sake of more commensurate visualizations.

We start by calculating the first derivative of $g(x)$ as:

$$\dot{g}(x) = 0.3\,x^2 + 0.4\,x + 0.3 \tag{6}$$

which allows us to write:

$$m = \dot{g}(x_0) = 0.3\,x_0^2 + 0.4\,x_0 + 0.3 = 1;$$
$$c = g(x_0) = 0.1\,x^3 + 0.2\,x^2 + 0.3\,x + 0.1 = 0.6;$$
$$\tilde{g}(x) = 1\,(x - 1) + 0.6 = x - 0.4$$

Figure 2 illustrates the original function (in blue) as well as its first-order approximation around $x_0 = 1$. It can be readily appreciated that function $\tilde{g}(x)$ provides as good approximations of $g(x)$ as x is close to x_0, especially within the interval $\Delta = [0.85, 1.15]$ (subjectively chosen for illustrative purposes).

To begin with, and as could have been expected, the exact derivative of $g(x)$ at x_0 can be immediately obtained as corresponding to $\dot{g}(x_0) = 1$.

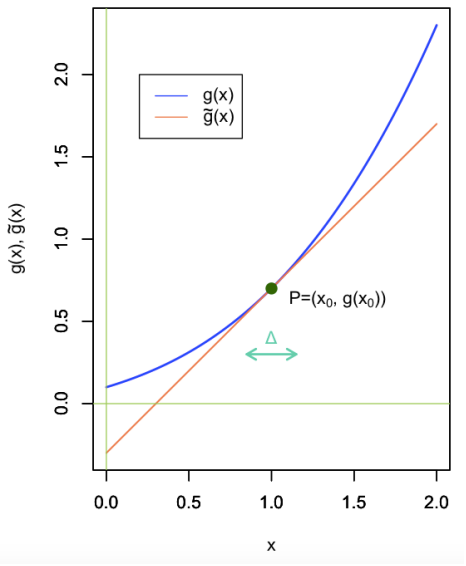

Figure 2: The function $g(x) = 0.1\,x^3 + 0.2\,x^2 + 0.3\,x + 0.1$ approximated as $\tilde{g}(x) = x - 0.4$ around the reference point $x_0 = 1$. The accuracy of the approximation increases as x becomes closer to x_0. A good overall approximation can be obtained within the indicated interval Δ.

In addition, we can also estimate the area $\tilde{A}$ of $g(x)$ along the interval Δ as:

$$\tilde{A} = \int_{x_i}^{x_f} g(x)\,dx \approx \int_{x_i}^{x_f} \tilde{g}(x)\,dx = \frac{|\Delta|}{2}\,[\tilde{g}(x_i) + \tilde{g}(x_f)]$$
$$\text{where: } |\Delta| = x_f - x_i$$

in which we used the simple formula for calculating the trapezium area.

Figure 3 illustrates the area to be estimated as corresponding to the area of the highlighted trapezium defined between the function $g(x)$ and the $x-$axis along the interval Δ.

In the particular case in which $\Delta = [0.85, 1.15]$, we have:

$$\tilde{A} = \frac{|\Delta|}{2}\,[\tilde{g}(0.85) + \tilde{g}(1.15)] = 2.1$$

Now, this is very close to the value ≈ 2.11125 obtained analytically (relative error of 0.53%), which substantiates how effective linear approximations can be, provided we operate sufficiently close to the reference point x_0.

Having obtained the approximation $\tilde{g}(x)$, another interesting possibility consists in defining a *new coordinate system* that adapts effectively to the original function $g(x)$ at x_0, as illustrated in Figure 4.

By "adapt" we mean that the new $\tilde{x}$ axis aligns with the tangent of the function at x_0, while having its origin at $P = (x_0, g(x_0))$. Informally speaking, it thus provide a representation of the function, as well as other elements

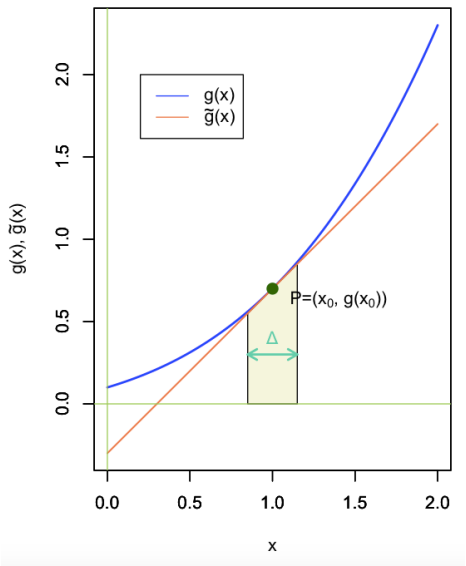

Figure 3: Illustration of using the approximation $\tilde{g}(x)$ for the estimation of the area comprised between the function $g(x)$ and the $x-$axis along the interval Δ. The obtained estimated area $\tilde{A} = 2.1$ is very close to the respective analytic value $A = 2.11125...$

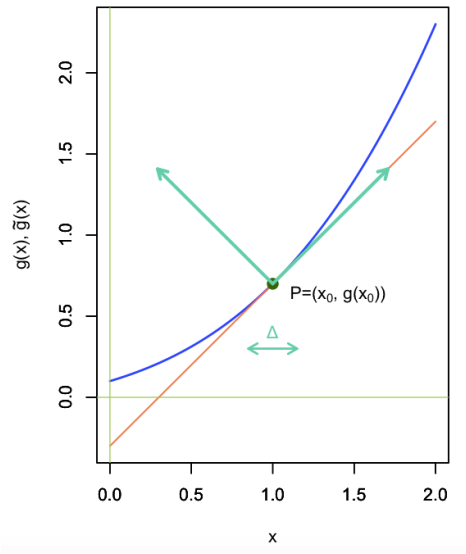

Figure 4: A new coordinate system $(\tilde{x}, \tilde{y})$ defined at $P = (x_0, g(x_0))$ by taking the tangent to the curve as being parallel to the first versor associated to the basis of the new coordinates. The second versor has been taken to be orthogonal to the first and oriented along the $y-$axis of the old system.

in the original space, as perceived by a nanoscopic elongated being placed at $P = (x_0, g(x_0))$ kept tangent to the original function (see Fig. 5).

Let us obtain this new coordinate system. First, we need to define the versors (vectors with unit magnitude) corresponding to the basis $\boldsymbol{b}$ of the new system, i.e. $\boldsymbol{b} = (\boldsymbol{b}_x, \boldsymbol{b}_y)$. Let us represent these two versors in the original coordinates as follows:

$$\boldsymbol{b}_x = (b_{xx}, b_{xy}) \tag{7}$$

$$\boldsymbol{b}_y = (b_{yx}, b_{yy}) \tag{8}$$

Let consider the vector $\boldsymbol{v}$ having $x_0 = 1$ for $x-$coordinate 1, and the slope m for $y-$coordinate. Importantly, m is here provided by the first-order approximation of the original function, i.e.:

$$\boldsymbol{v} = \left(1, m = \frac{dg}{dx}\Big|_{x_0} = 1\right)$$

This vector is parallel to the sought versor $\boldsymbol{b}_x$, which can therefore be obtained by normalizing $\boldsymbol{v}$ so as to have unit magnitude:

$$\boldsymbol{b}_x = \frac{\boldsymbol{v}}{||\boldsymbol{v}||} = \left(\frac{\sqrt{2}}{2}, \frac{\sqrt{2}}{2}\right)$$

Interestingly, though the the other versor $\boldsymbol{b}_y$ is orthogonal to the just determined $\boldsymbol{b}_x$, it cannot be determined in a unique manner, given that there are two such orthogonal versors, oriented toward opposite directions. In the case of our particular example, we take the upward direction.

Therefore, in order to determine the second versor $\boldsymbol{b}_y$ of our new basis, we start with the vector:

$$\boldsymbol{r} = (r_x, 1)$$

and them apply the orthogonality restriction, leading to:

$$\langle \boldsymbol{r},\ \boldsymbol{b}_x \rangle = 0 \implies r_x\, b_{xx} + (1)\, b_{yy} = 0 \implies$$

$$\implies r_x = -\frac{b_{yy}}{b_{xx}} = -\frac{\sqrt{2}/2}{\sqrt{2}/2} = -1$$

so that:

$$\boldsymbol{r} = (-1, 1)$$

Thus, the second versor can be obtained by normalizing $\boldsymbol{r}$ as:

$$\boldsymbol{b}_y = \frac{\boldsymbol{r}}{||\boldsymbol{r}||} = \left(-\frac{\sqrt{2}}{2}, \frac{\sqrt{2}}{2}\right)$$

The versors constituting the basis of the new system of coordinates can then be summarized as:

$$\boldsymbol{b}_x = \left(\frac{\sqrt{2}}{2}, \frac{\sqrt{2}}{2}\right)$$

$$\boldsymbol{b}_y = \left(-\frac{\sqrt{2}}{2}, \frac{\sqrt{2}}{2}\right)$$

The *basis transformation* from the old Cartesian basis $\boldsymbol{b}$ to the new, rotated basis $\tilde{\boldsymbol{b}}$ can now be performed (e.g. [3]) as follows:

$$\boxed{\tilde{\boldsymbol{b}} = \boldsymbol{b}\, A} \tag{9}$$

where:

$$\boldsymbol{b} = [\hat{i}\ \hat{j}]$$
$$\tilde{\boldsymbol{b}} = [\boldsymbol{b}_x\ \boldsymbol{b}_y]$$

and the respective transformation matrix A corresponds to:

$$A = \begin{bmatrix} \uparrow & \uparrow \\ \boldsymbol{b}_x & \boldsymbol{b}_x \\ \downarrow & \downarrow \end{bmatrix} = \begin{bmatrix} \frac{\sqrt{2}}{2} & -\frac{\sqrt{2}}{2} \\ \frac{\sqrt{2}}{2} & \frac{\sqrt{2}}{2} \end{bmatrix} \tag{10}$$

The coordinates $\tilde{\boldsymbol{v}} = (\tilde{x}$ and $\tilde{y})$ in the new system of coordinates associated to the point P can the be expressed in terms of the old coordinates $\boldsymbol{v} = (x$ and $y)$ by translating the old coordinate to $(x_0, g(x_0)$ and then performing the basis transformation according to A (e.g. [3]), which can be summarized as:

$$\boxed{\tilde{\boldsymbol{v}} = A^{-1}\,[\boldsymbol{v} - \boldsymbol{c}]} \tag{11}$$

where:

$$\boldsymbol{c} = \begin{bmatrix} x_0 \\ g(x_0) \end{bmatrix} = \begin{bmatrix} 1 \\ 0.7 \end{bmatrix}$$
$$A^{-1} = \begin{bmatrix} \frac{\sqrt{2}}{2} & \frac{\sqrt{2}}{2} \\ -\frac{\sqrt{2}}{2} & \frac{\sqrt{2}}{2} \end{bmatrix}$$

Equation 11 corresponds to an *affine transformation*, which has general form:

$$\tilde{\boldsymbol{r}} = B\,\boldsymbol{r} + \boldsymbol{c} \tag{12}$$

This type of transformation involves a *linear transformation* $B\,\boldsymbol{r}$ plus a translation by $\boldsymbol{c}$.

Figure 5 illustrates the representation in the new system of coordinates of the curve derived from the function $g(x)$. Observe how well the new coordinate $\tilde{x}$ aligns with the original function, therefore "following" the respectively defined curve.

It is interesting to realize that the obtained reference frame is completely independent of the choice between orthonormal coordinate systems to represent the original function, reflecting only the shape of the curve at a small neighborhood around the reference point.

In addition, it is important to keep in mind that linear or affine transformations of a curve defined by a single-variable function (as $g(x)$ in the above example) may no longer correspond to functions in the new coordinate system, in the sense that two or more images my become

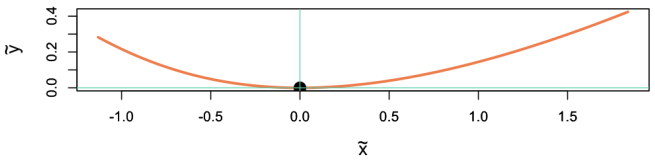

Figure 5: The representation in the new coordinate system $\tilde{x}, \tilde{y})$ of the curve defined by function $g(x)$ in the considered example. The new coordinate axis $\tilde{x}$ aligns effectively with the curve, especially in the neighborhood around the reference point P.

associated to a single abscissae value. The more general *parametric representation* or curves, to be addressed in Section 4, can be adopted in order to transform one-variable functions into respective, more versatile, parametric curves.

Now, let us suppose we had a set of fanning curves in our original system, as illustrated in Figure 6, and that we are interested in defining a new system of coordinates that not only has its orientation aligned with the tangent of the curves, but also could expand them so as to provide a more detailed representation. More specifically, let us focus on the set of curves at the right-hand side of point P (a similar approach can be developed for the other side).

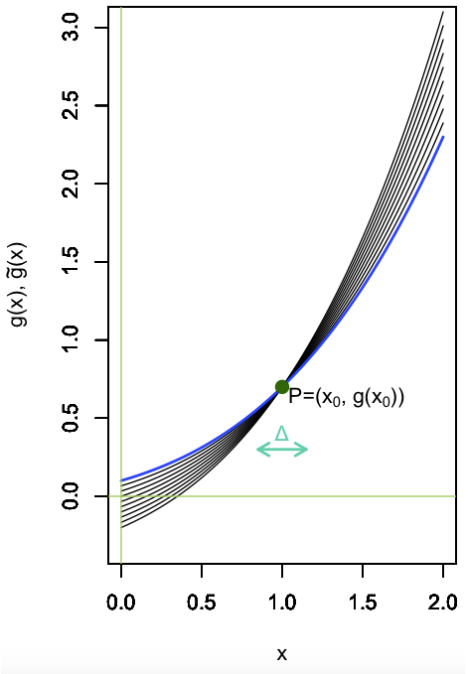

Figure 6: How can a set of several curves be better represented and visualized by a new system of coordinates? The previous function $g(x)$ is shown in blue, for reference.

A suitable new, *sheared* system of coordinates is illustrated in green in Figure 7. Observe that the respective versors corresponding to the new axes have different sizes,

and are not orthonormal, as a means to better span the fanning curves.

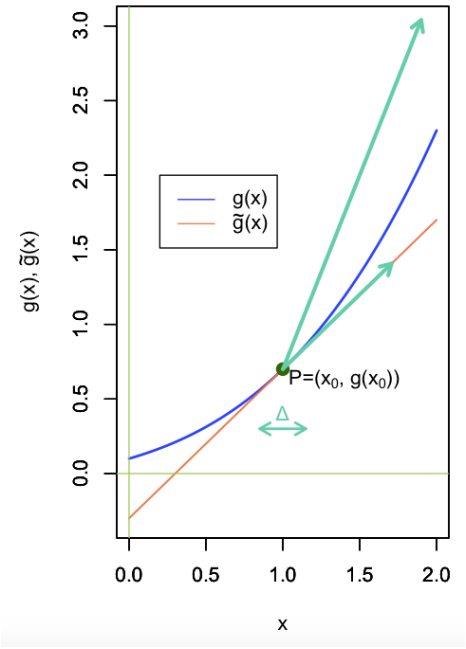

Figure 7: A possible new system of coordinates that, by being *sheared*, can provided an expanded representation of the fanning curves extending from P towards the right-hand side of the set of curves.

In order to obtain this new system, we use the same versor $\boldsymbol{b}_x$ as before, while a new vector is used as second-element of the now non-orthonormal basis. For instance, we can choose:

$$\boldsymbol{b}_x = \left(\frac{\sqrt{2}}{2}, \frac{\sqrt{2}}{2}\right)$$
$$\boldsymbol{b}_y = (0.90, 2.34)$$

This somewhat subjective choice of new basis vectors determines the basis transformation matrix as:

$$A = \begin{bmatrix} \frac{\sqrt{2}}{2} & 0.90 \\ \frac{\sqrt{2}}{2} & 2.34 \end{bmatrix}$$

which has respective inverse given as:

$$A^{-1} = \begin{bmatrix} 2.298 & -0.884 \\ -0.69 & 0.694 \end{bmatrix}$$

By using Equation 12, we can now obtain a visualization of how the fanning curves appear as represented in the new coordinate system, which is depicted in Figure 8. Observe how the curves have become more well-separated one another, allowing more effective representation and visualization. Although these curves can no longer be guaranteed to be expressible as functions of the type $\tilde{y} = h(\tilde{x})$, they can be translated into respective parametric curves if necessary.

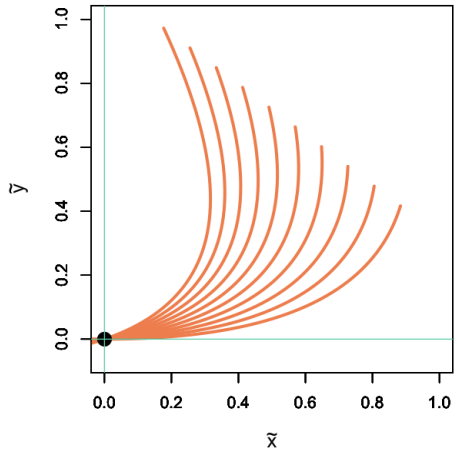

Figure 8: The fanning curves as represented in the new, sheared system of coordinates result suitably expanded, allowing more effective representation and visualization. Observe that these curves can no longer be guaranteed to correspond to functions of the type $\tilde{y} = h(\tilde{x})$, since multiple images of a same abscissae may be involved. If necessary, these curves can be properly represented in terms of parametric curves.

The example above concludes our presentation of how linear approximations of a function or curve (or set of curves, as well as points) can be obtained by considering the first-order Taylor expansion of one of the functions, taken as reference. As illustrated, this approach presents remarkable potential for performing several important mathematical operations in terms of the simplified first-order approximations. Observe that, though we were mainly restricted to a third-degree polynomial, other more intricate functions can be readily considered, provided we can calculate their first derivative at the point P to be taken as reference.

Among the many tasks that can be performed in simplified manner in terms of the first-order approximations, we have: (i) estimating areas; (ii) extrapolation around a reference point; and (iii) definition of new bases and systems of coordinates. In the latter case, which has been here illustrated respectively to orthonormal and sheared new coordinate systems, we verified that they can account for interesting representations that adapts to the local geometry of the curve around P, as well as for expanding regions through shearing.

One important related issue concerns how operations/measurements such as the inner product, angles and magnitudes are affected by these coordinate changes. While orthonormal new systems will not influence most of these operations and measurements, sheared new systems modify several of them, though some operations and

measurements can be identified as being *invariant* to the implemented transformation (e.g. [3]).

In the following section, we present the important concept of the *Jacobian* of a transformation and its application to generalize the first-order expansion, discussed here respectively to single-variable functions in $2D-$spaces, to mathematical structures in higher dimensional spaces. The good news is that most of this can be done in direct analogy to what we discussed and implemented in the present section.

3 The Gradient as a First-Order Multivariate Operator

Though in this section we shall focus on $\mathbb{R}^3$, the respective discussion and results can be immediately translated to smaller or higher dimensional spaces.

A scalar field $\psi(x,y,z)$ mapping points (x,y,z) of $\mathbb{R}^3$ into $\mathbb{R}$, is said to be *differentiable* in case we can obtain its *first-order multdimensional partial derivatives*:

$$\frac{\partial\,\psi(x,y,z)}{\partial x};\quad \frac{\partial\,\psi(x,y,z)}{\partial y};\quad \frac{\partial\,\psi(x,y,z)}{\partial z} \tag{13}$$

which will be henceforth abbreviated as:

$$\frac{\partial\,\psi}{\partial x};\quad \frac{\partial\,\psi}{\partial y};\quad \frac{\partial\,\psi}{\partial z} \tag{14}$$

Each of these partial derivatives indicates how the scalar field values vary as a consequence of respective *differential* displacements dx, dy, and dz. As such, the partial derivatives are respective to each adopted system of coordinates.

In $\mathbb{R}^2$, the plane defined as $\psi(x,y) = 2x - 3y + 1$ will have the following partial first derivatives:

$$\frac{\partial\,\psi}{\partial x} = 2;\quad \frac{\partial\,\psi}{\partial y} = -3$$

However, when the coordinates are changed as:

$$\left[\begin{array}{c}\tilde{x}\\ \tilde{y}\end{array}\right] = A^{-1}\left[\begin{array}{c}x\\ y\end{array}\right] = \left[\begin{array}{cc}\frac{\sqrt{2}}{2} & \frac{\sqrt{2}}{2}\\ -\frac{\sqrt{2}}{2} & \frac{\sqrt{2}}{2}\end{array}\right]\left[\begin{array}{c}x\\ y\end{array}\right] \tag{15}$$

so that:

$$\left[\begin{array}{c}x\\ y\end{array}\right] = A\left[\begin{array}{c}\tilde{x}\\ \tilde{y}\end{array}\right] = \left[\begin{array}{cc}\frac{\sqrt{2}}{2} & -\frac{\sqrt{2}}{2}\\ \frac{\sqrt{2}}{2} & \frac{\sqrt{2}}{2}\end{array}\right]\left[\begin{array}{c}\tilde{x}\\ \tilde{y}\end{array}\right] \tag{16}$$

it follows that:

$$\left\{\begin{array}{l} x = \frac{\sqrt{2}}{2}\,\tilde{x} - \frac{\sqrt{2}}{2}\,\tilde{y}\\ y = \frac{\sqrt{2}}{2}\,\tilde{x} + \frac{\sqrt{2}}{2}\,\tilde{y}\end{array}\right. \tag{17}$$

which can be used to express the plane in the new coordinate system as:

$$\begin{aligned}&\psi(x,y) = 2\,x - 3\,y + 1 =\\ &= 2\left(\frac{\sqrt{2}}{2}\,\tilde{x} - \frac{\sqrt{2}}{2}\,\tilde{y}\right) - 3\left(\frac{\sqrt{2}}{2}\,\tilde{x} + \frac{\sqrt{2}}{2}\,\tilde{y}\right) + 1 =\\ &= -\frac{\sqrt{2}}{2}\,\tilde{x} - 5\,\frac{\sqrt{2}}{2}\,\tilde{y} + 1 = \psi(\tilde{x},\tilde{y})\end{aligned} \tag{18}$$

Thus, the partial derivatives in the new coordinate system result as:

$$\frac{\partial\,\tilde{\psi}}{\partial\tilde{x}} = -\frac{\sqrt{2}}{2};\quad \frac{\partial\,\tilde{\psi}}{\partial\tilde{y}} = -\frac{5\sqrt{2}}{2}$$

which, as expected, are distinct from the partial derivatives in the old system of coordinates.

Though both old and new systems of coordinates in the previous example were associated to orthonormal bases, it is also interesting to consider the gradient in a sheared coordinate system. Let us illustrate this interesting possibility by using the following direct transformation matrix instead of the previous one:

$$A = \left[\begin{array}{cc}1 & 2\\ -1 & 1\end{array}\right] \tag{19}$$

Therefore, the old coordinates can be expressed respectively to the new coordinates as:

$$\left\{\begin{array}{l} x = \tilde{x} + 2\,\tilde{y}\\ y = -\tilde{x} + \tilde{y}\end{array}\right. \tag{20}$$

From which the equation of the plane in the new coordinate can be obtained as follows:

$$\begin{aligned}&\psi(x,y) = 2\,x - 3\,y + 1 =\\ &= 2\,(\tilde{x} + 2\tilde{y}) - 3\,(-\tilde{x} + \tilde{y}) + 1 =\\ &= 5\tilde{x} + \tilde{y} + 1 = \psi(\tilde{x},\tilde{y})\end{aligned} \tag{21}$$

which has respective partial derivatives corresponding to:

$$\frac{\partial\,\tilde{\psi}}{\partial\tilde{x}} = 5;\qquad \frac{\partial\,\tilde{\psi}}{\partial\tilde{y}} = 1$$

which are again different from the partial derivatives in the old system.

Observe that the partial derivatives are calculated in the same manner as in an orthonormal system, even though $\tilde{x}$ and $\tilde{y}$ are respective to a sheared basis which is neither orthogonal nor with vectors normalized to unit magnitude. That is because the partial derivatives are taken along each of the axes, irrespectively on if they are sheared, normalized, or not. However, distinct results will likely result in each of these cases.

We could also have used the multivariate chain rule to estimate the new derivatives, i.e.:

$$\frac{\partial \psi}{\partial \tilde{x}} = \frac{\partial \psi}{\partial x}\frac{\partial x}{\partial \tilde{x}} + \frac{\partial \psi}{\partial y}\frac{\partial y}{\partial \tilde{x}} = (2)(1) + (-3)(-1) = 5;$$
$$\frac{\partial \psi}{\partial \tilde{y}} = \frac{\partial \psi}{\partial x}\frac{\partial x}{\partial \tilde{y}} + \frac{\partial \psi}{\partial y}\frac{\partial y}{\partial \tilde{y}} = (2)(2) + (-3)(1) = 1$$

therefore confirming the above results.

The vector defined by the three partial derivatives of a scalar field $\psi(x, y, z)$ at a point (x, y, z) corresponds to the *gradient* of that field, which can thus be expressed as:

$$\boldsymbol{\nabla}\psi = \frac{\partial \psi}{\partial x}\,\boldsymbol{b}_x + \frac{\partial \psi}{\partial y}\,\boldsymbol{b}_y + \frac{\partial \psi}{\partial z}\,\boldsymbol{b}_z \tag{22}$$

where the canonical basis $[\hat{i}, \hat{j}, \hat{k}]$ is often (but not necessarily) chosen for $\boldsymbol{b}$ of $\mathbb{R}^3$.

Let us now consider the *dot product* of two vectors $\boldsymbol{v}$ and $\boldsymbol{r}$ as:

$$\boldsymbol{v} \cdot \boldsymbol{r} = \langle \boldsymbol{v} \cdot \boldsymbol{r} \rangle = \boldsymbol{v}^T\,\boldsymbol{r} \tag{23}$$

Though the scalar product is not preserved when transformed into sheared coordinates (e.g. undergoing linear transformations), it can be nevertheless be defined as above for each of the respective coordinate systems. In fact, the *inner product* can be though of as a more general concept (satisfying some conditions), with the dot product being a particular case.

Interestingly, the partial derivatives can be themselves understood as an *operator*, which allows to express the gradient in the following alternative manner involving the dot product:

$$\boldsymbol{\nabla}\psi = \begin{bmatrix} \frac{\partial}{\partial x}\boldsymbol{b}_x & \frac{\partial}{\partial y}\boldsymbol{b}_y & \frac{\partial}{\partial z}\boldsymbol{b}_z \end{bmatrix} \begin{bmatrix} \psi \\ \psi \\ \psi \end{bmatrix} = \boldsymbol{\nabla} \cdot \boldsymbol{\psi} \tag{24}$$

observe that the gradient operator will be treated as a row vector, while traditional vectors will be represented as column vectors.

Let us know briefly consider how the gradient *operator* is modified as a consequence of a linear basis transformation.

The terms *covariant* and *contravariant* are often employed in order to express how a structure (e.g. a vector) or an operation (e.g. differentiation) change when under a basis transformation by respective matrix A (e.g. [3]). In case the entity is transformed in agreement with A, the change is said to be *covariant*; otherwise, in case the change goes with the inverse of A, it is said to be *contravariant*.

Traditional column vectors are contravariant, but horizontal vectors are covariant, and correspond to *co-vectors*. Distinct bases are used to express vectors and covectors: respectively the "direct" basis, and the *dual basis*. In the case of orthonormal systems, these two bases are identical, hence vectors are rarely distinguished from co-vectors. However, in more general sheared spaces the two bases are distinct and have distinct transformation rules (e.g. [3]).

Because the resulting gradient of a scalar field is *covariant* (e.g. [3]), we can obtain its value in a linearly transformed system as:

$$\boxed{\tilde{\boldsymbol{\nabla}}\psi = \boldsymbol{\nabla}\psi\, A} \tag{25}$$

In the case of the previous example involving an orthonormal basis, we would have:

$$\tilde{\boldsymbol{\nabla}}\psi = \begin{bmatrix} \frac{\partial \tilde{\psi}}{\partial \tilde{x}} & \frac{\partial \tilde{\psi}}{\partial \tilde{y}} \end{bmatrix} =$$
$$= \begin{bmatrix} 2 & -3 \end{bmatrix} \begin{bmatrix} \frac{\sqrt{2}}{2} & -\frac{\sqrt{2}}{2} \\ \frac{\sqrt{2}}{2} & \frac{\sqrt{2}}{2} \end{bmatrix} = \begin{bmatrix} -\frac{\sqrt{2}}{2} & -\frac{5\sqrt{2}}{2} \end{bmatrix}$$

and, in the case of the sheared basis:

$$\tilde{\boldsymbol{\nabla}}\psi = \begin{bmatrix} 2 & -3 \end{bmatrix} \begin{bmatrix} 1 & 2 \\ -1 & 1 \end{bmatrix} = \begin{bmatrix} 5 & 1 \end{bmatrix}$$

The *total derivative* of the scalar field $\psi(x, y, z)$ corresponds to how much that field changes as a consequence of incremental displacements (i.e. *differentials*) dx, dy, and dz along each of the respective axes. The total derivative can be compactly expressed in terms of the following dot product:

$$\boldsymbol{d\psi} = \begin{bmatrix} \frac{\partial \psi_x}{\partial x} & \frac{\partial \psi_x}{\partial y} & \frac{\partial \psi_x}{\partial z} \end{bmatrix} \begin{bmatrix} dx \\ dy \\ dz \end{bmatrix} \tag{26}$$

The *directional* derivative of a scalar field $\psi(x, y, z)$, respectively to a versor $\hat{\boldsymbol{u}} = (u_x, u_y, u_z)$ at a reference point $\boldsymbol{v}_0 = (x_0, y_0, z_0)$, can be expressed as:

$$\boldsymbol{\nabla}\psi\big|_{\hat{\boldsymbol{u}}, \boldsymbol{v}_0} = \left\langle \boldsymbol{\nabla}\psi\big|_{\boldsymbol{v}_0}, \hat{\boldsymbol{u}} \right\rangle = \begin{bmatrix} \frac{\partial \psi_x}{\partial x} & \frac{\partial \psi_x}{\partial y} & \frac{\partial \psi_x}{\partial z} \end{bmatrix} \begin{bmatrix} u_x \\ u_y \\ u_z \end{bmatrix} \tag{27}$$

This derivative quantifies how much the scalar field changes along the orientation specified by the versor $\boldsymbol{u}$ at the reference point $\boldsymbol{v}_0$.

As discussed in this section, though constituting a first-order concept, the gradient can be applied to obtain information about a variety of properties of scalar fields, including the direction of their largest variation, the increase respective to small displacements, as well as the incremental variation along a given orientation.

4 $2D$ and $3D$ Parametric Curves

In Section 2, we started our study of first-order approximation with a single-variable function which was transformed into new bases. As discussed in that section, this

can lead to a transformed curve that does not correspond to a valid function in the transformed space, a problem that can e avoided in case we consider parametric curves from the beginning, instead of functions, which has an additional advantage of allowing a wider range or curves (and not only those described as a function) to be considered.

In this section, we introduce the concept of parametric curves in $2D$ and $3D$ and then revisit the first-order approximation from this perspective. As we shall see, the adoption of parametric curves has another advantage in which an orthonormal system of coordinate can be directly assigned to all the points along the curve that do not correspond to straight line segments. The problem with the latter type of curves is that they only have a well-defined tangent, so that the other axes have to be decided by considering criteria extrinsic to the curve.

A parametrized curve $g(t)$ of a free variable $t \in [a, b]$ can be expressed as:

$$\boldsymbol{g}(t) = (g_x(t), g_y(t), g_z(t))$$

In case they exist, its first and second derivatives with respect to time then correspond to:

$$\begin{cases} \dot{\boldsymbol{g}}(t) = (\dot{g}_x(t), \dot{g}_y(t), \dot{g}_z(t)) \\ \ddot{\boldsymbol{g}}(t) = (\ddot{g}_x(t), \ddot{g}_y(t), \ddot{g}_z(t)) \end{cases} \tag{28}$$

As with single-variable functions $g(x)$, parametric curves $\boldsymbol{g}(t)$ on a generic parameter t can be approximated in terms of their first-order derivatives by applying the Taylor series on the respective components, i.e.:

$$\boxed{\begin{cases} g_x(t)\big|_{t_0} \approx g_x(t_0) + \dot{g}_x(t_0)\ (t - t_0) \\ g_y(t)\big|_{t_0} \approx g_y(t_0) + \dot{g}_y(t_0)\ (t - t_0) \\ g_z(t)\big|_{t_0} \approx g_z(t_0) + \dot{g}_z(t_0)\ (t - t_0) \end{cases}}. \tag{29}$$

Let us illustrate the first-order approximation of a parametric curve respectively to the following particular curve:

$$\begin{cases} g_x(t) = \sin(t) + 2\,\sin(2\,t) \\ g_y(t) = \cos(t) - 2\,\cos(2\,t) \\ g_z(t) = \sin(2\,t) \end{cases}$$

The first derivatives of its components are as follows:

$$\begin{cases} \dot{g}_x(t) = \cos(t) + 4\,\cos(2\,t) \\ \dot{g}_y(t) = -\sin(t) + 4\,\cos(2\,t) \\ \dot{g}_z(t) = -2\,\cos(2\,t) \end{cases}$$

By substituting these derivatives in Equation 29 for $t = 1.7$, we obtain the first order approximation shown as a dashed red line in Figure 9.

The *differential arc length* of $g(t)$ can be expressed as:

$$ds = \sqrt{\dot{x}^2 + \dot{y}^2 + \dot{z}^2}\,dt \tag{30}$$

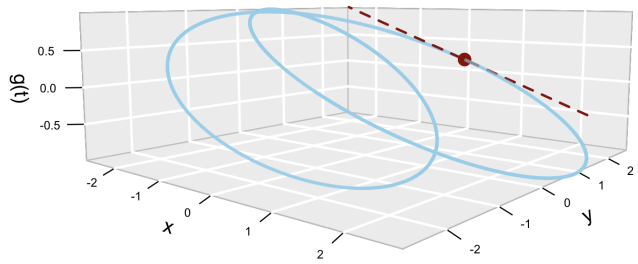

Figure 9: A parametric curve and the first-order approximation for $t = 1.7$, implying $(0.480, 1.80, 0.25)$, shown as the dashed red straight line.

so that the accumulated arc-length from the beginning $g(t_i)$ of the curve can be calculated as:

$$s(\tau) = \int_{t_i}^{\tau} ds = \int_{t_i}^{\tau} \sqrt{\dot{x}^2 + \dot{y}^2 + \dot{z}^2}\,dt \tag{31}$$

Parametric curves $\boldsymbol{g}(s)$ having parameter corresponding to the arc-length along the curve are particularly important, being said to be in *arc-length parametrization*.

Let one such curve be represented as:

$$\boldsymbol{g} = (g_x(s), g_y(s), g_z(s))$$

It follows that:

$$\begin{cases} \boldsymbol{t}(s) = \dot{\boldsymbol{g}}(s) = (\dot{g}_x(s), \dot{g}_y(s), \dot{g}_z(s)), \quad \textit{with: } ||\boldsymbol{t}(s)|| = 1 \\ \tilde{\boldsymbol{n}}(s) = \ddot{\boldsymbol{g}}(s) = (\ddot{g}_x(s), \ddot{g}_y(s), \ddot{g}_z(s)) \end{cases} \tag{32}$$

where $\tilde{n}(s)$ is normal to the curve. One of the important implications of arc-length parametrization is that, given that the velocity associated to the tangent $\boldsymbol{t}(s)$ has constant magnitude, the effect of the normal field becomes restricted to changing *only the orientation* of the velocity.

Though $\tilde{n}(s)$ is a field normal to the curve, it is not necessarily a versor (unit length). The normalized normal field can thus be obtained as:

$$\boldsymbol{n}(s) = \frac{\tilde{\boldsymbol{n}}(s)}{||\tilde{\boldsymbol{n}}(s)||} = \frac{\ddot{\boldsymbol{g}}(s)}{||\ddot{\boldsymbol{g}}(s)||} \tag{33}$$

The two vector functions $\boldsymbol{t}(s)$ and $\boldsymbol{n}(s)$ of the arc-length parameter s are centrally important, corresponding to the *tangent* and *normal* fields along the curve.

In the case of $\mathbb{R}^2$, at the portions of the curve which do not correspond to straight line segments, these two vector functions provide a natural choice to be taken as a basis underlying respective orthonormal systems of coordinates extending continuously along all the points of the curve. For instance, only the tangent filed can be defined for a straight line, implying the normal field to be imposed through some additional restriction.

As discussed above, $\boldsymbol{t}(s)$ and $\boldsymbol{n}(s)$ therefore implement in an effective manner the task of obtaining coordinate systems that adapt locally to the curve, which had been preliminary considered in Section 2.

The idea of assigning locally adapted systems of coordinates along a curve can be extended to higher dimensional mathematical structures, such as surfaces and volumes. These approaches are systematically studied in differential geometry and tensor calculus.

In the case of $\mathbb{R}^3$ we need a third versor to complete the coordinate systems to be assigned to the curve. This third vector can be readily obtained from $\boldsymbol{t}(s)$ and $\boldsymbol{n}(s)$ in terms of their cross product, i.e.:

$$\boldsymbol{b}(s) = \boldsymbol{t}(s) \times \boldsymbol{n}(s) \tag{34}$$

where we chose to have a *right-hand* coordinate system. The vector $\boldsymbol{b}$ is a *versor* called the *binormal vector*. Observe that the cross product of two non-parallel versors is necessarily a versor.

So, provided the curve is differentiable and do not correspond to a straight line, the above vector functions of s constitute a natural choice for an adaptable orthonormal basis $[\boldsymbol{t}(s), \boldsymbol{n}(s), \boldsymbol{b}(s)]$. This orthonormal system of coordinates is know as the *Frenet-Serret trihedron*. It can be shown that the derivatives of these vector functions can be expressed as:

$$\frac{d\boldsymbol{t}}{ds} = \kappa\, \boldsymbol{n} \tag{35}$$

$$\frac{d\boldsymbol{n}}{ds} = -\kappa\, \boldsymbol{t} - \tau \boldsymbol{b} \tag{36}$$

$$\frac{d\boldsymbol{b}}{ds} = \tau\, \boldsymbol{n} \tag{37}$$

which are the *Frenet-Serret* vector derivatives of $\boldsymbol{g}(s)$.

In the above equations, $\tau(s)$ is the *torsion* of the curve, and $\kappa(s)$ is its *curvature*, defined as:

$$\kappa(s) = ||\ddot{\boldsymbol{g}}(s)|| = ||\dot{\boldsymbol{t}}(s)|| = ||\tilde{\boldsymbol{n}}(s)|| \tag{38}$$

In case the curve parameter t does not correspond to the arc-length, it is still possible to obtain the respective curvature by using the expression:

$$\kappa(t) = \frac{\dot{g}_x \ddot{g}_y - \dot{g}_y \ddot{g}_x}{\left(\dot{g}_x^2 + \dot{g}_y^2\right)^{3/2}} \tag{39}$$

It can be shown that for any $\kappa(s)$ and $\tau(s)$, a parametric curve $g(s)$ can be found that is characterized by those two properties.

Observe that, although the first-order tangent approximation to the curve is employed in the Frenet trihedron, that frame also involves second-order elements, namely the normal field obtained from the second derivative of the original parametric curve. Thus, by incorporating additional information about the original parametric curve, the consideration of the second derivative leads to a reference frame that is even more adapted to the local curve shape.

Though theoretically appealing and effective, in practice it often constitutes a challenge to place a curve in a generic parameter t into arc-length parametrization. Nevertheless, the above results provide a powerful resource in theoretic-analytical aspects of differential geometry and related areas.

In addition, the Frenet trihedron *at a specific* reference point (x_0, y_0, z_0) can be obtained in a relatively simple manner for a regular curve in generic parametrization by obtaining non-normalized tangent and normal fields, and then normalizing them.

This approach is possible because the following vector fields obtained more directly from a curve not necessarily in arc-length parametrization *will also be* tangent and normal, respectively, to the curve, though not necessarily having unit length:

$$\dot{\boldsymbol{g}}(t) = \frac{d\boldsymbol{g}(t)}{dt} \tag{40}$$

$$\ddot{\boldsymbol{g}}(t) = \frac{d^2\boldsymbol{g}(t)}{dt^2} \tag{41}$$

We will illustrate the above approach respectively to the following parametric curve:

$$\boldsymbol{g}: \quad \begin{cases} g_x(x,y,z) = 3t \\ g_y(x,y,z) = (e^t - 1)\, \cos 20t \\ g_z(x,y,z) = (e^t - 1)\, \sin 20t \end{cases} \tag{42}$$

The respective first derivatives are:

$$\begin{cases} \dot{g}_x = 3 \\ \dot{g}_y = e^t \cos(f_0\, t) - 20 \sin(f_0\, t)\, (e^t - 1) \\ \dot{g}_z = e^t \sin(f_0\, t) + 20 \cos(f_0\, t)\, (e^t - 1) \end{cases}$$

and the second derivatives correspond to:

$$\begin{cases} \dot{g}_x = 0 \\ \dot{g}_y = -399 e^t \cos(f_0\, t) - 40 e^t \sin(f_0\, t) + 400 \cos(f_0\, t) \\ \dot{g}_z = -399 e^t \sin(f_0\, t) + 40 e^t \cos(f_0\, t) + 400 \sin(f_0\, t) \end{cases}$$

The Frenet trihedron obtained fro $T = 0.45$, shown in Figure 10, was calculated as:

$$\boldsymbol{t} = \begin{bmatrix} 0.252 \\ -0.515 \\ -0.818 \end{bmatrix}; \quad \boldsymbol{n} = \begin{bmatrix} 0.000 \\ 0.865 \\ -0.501 \end{bmatrix}; \quad \boldsymbol{b} = \begin{bmatrix} 0.967 \\ 0.126 \\ 0.219 \end{bmatrix}$$

Figure 10 shows the parametric curve in Equation 42, as well as its respective Frenet trihedron obtained for $t = 0.45$. It is interesting to observe how the obtained frame adapts along the tangent and normal to this $3D$ parametric curve, which was indeed our initial objective. A specific Frenet trihedron can be for each of the possible points of reference defined by respective values of t, therefore covering the whole curve.

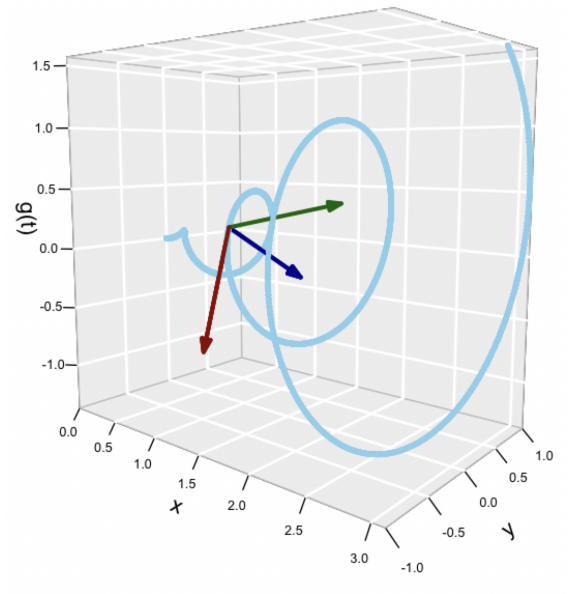

Figure 10: The parametric curve $g(t)$ in Eq. 42 and the Frenet trihedron obtained at the reference point $(g_x(0.5), g_y(0.45), g_z(0.45)$. The tangent, normal, and binormal vectors are shown in red, blue and green, respectively.

5 Multivariate Functions and Surfaces

A function of two variables can be understood as a *scalar field* on $\mathbb{R}^2$, i.e.:

$$g(x,y) : (x,y) \in \mathbb{R}^2 \longrightarrow g(x,y) = z \in \mathbb{R} \tag{43}$$

which is also known as a *graph representation* of the function because it involves the graph $z = g(x,y)$.

As with single-variable functions, a scalar field can be approximated in the neighborhood of one of its domain points (x_0, y_0) in terms of the respective Taylor series:

$$\boxed{g(x,y)\big|_{\boldsymbol{v}_0} \approx g(x_0,y_0) + [\boldsymbol{\nabla}(x_0,y_0)]^T \cdot [(x,y) - (x_0,y_0)]} \tag{44}$$

where $\boldsymbol{v}_0 = (x_0, y_0)$.

The above concepts can be immediately extended to higher dimensions:

$$g(\boldsymbol{v}) : \boldsymbol{v} \in \mathbb{R}^N \longrightarrow g(\boldsymbol{v}) = z \in \mathbb{R} \tag{45}$$

where $\boldsymbol{v} = (x_1, x_2, \ldots, x_N)$.

$$\boxed{g(\boldsymbol{v})\big|_{\boldsymbol{v}_0} \approx g(\boldsymbol{v}_0) + [\boldsymbol{\nabla}(\boldsymbol{v}_0)]^T \cdot (\boldsymbol{v} - \boldsymbol{v}_0)} \tag{46}$$

where $\boldsymbol{v}_0 = (x_{1,0}, x_{2,0}, \ldots, x_{N,0})$.

We illustrate the first order approximation of two-variable functions respectively to the following paraboloid:

$$z = y(x,y) = -x^2 - y^2 \tag{47}$$

whose first derivatives can be readily expressed as follows;

$$\frac{\partial z}{\partial x} = -2x$$
$$\frac{\partial z}{\partial y} = -2y$$

Thus, the first-order approximation of this function around the reference point $(x_0, y_0) = (1,1)$ can be written as:

$$\begin{aligned}
&g(x,y)\big|_{(x_0,y_0)} \approx \\
&\approx g(x_0,y_0) + \boldsymbol{\nabla}^T g\big|_{(x_0,y_0)} \cdot [(x,y) - (x_0,y_0)] = \\
&= g(x_0,y_0) + (-2x_0 \;\; -2y_0) \cdot [(x,y) - (1,1)] = \\
&= g(1,1) + (-2,-2) \cdot (x-1, y-1) = \\
&= -2 - 2x - 2y + 4 = -2x - 2y + 2
\end{aligned}$$

which corresponds to the equation of the plane that is tangent to the paraboloid at the reference point $(x_0, y_0) = (1,1)$, as illustrated in Figure 11.

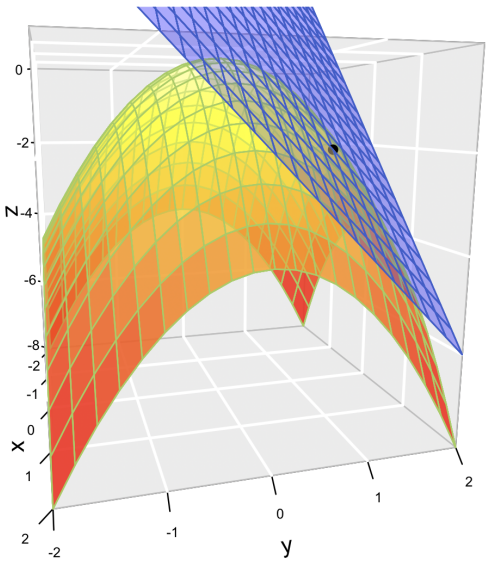

Figure 11: The paraboloid corresponding to Equation 47 and the plane that is tangent to it at the point $(1,1)$. This plane, which corresponds to the first-order respective representation of the original multivariate function, provides a good approximation of that function around the reference point.

6 Implicit Representations

We have approached curves in terms of single-variable functions (called a *graph* representation) and parametric forms. There is a third, equally interesting manner to

define a $1D$ curve in $\mathbb{R}^2$, which consists of understanding that every point that satisfies a given *relation*, *restriction*, or *constraint* belongs to the curve. A restriction is simply an equation of the type:

$$g(x,y) = 0, \quad (x,y) \in \mathbb{R}^2;$$
$$g(x,y,y) = 0, \quad (x,y,z) \in \mathbb{R}^3;$$

which corresponds to an *implicit curve*, given that it is not expressed in terms of the graph forms $y = f(x)$ or $z = g(x,y)$. Observe that $g(x,y)$ can be understood as a *scalar field* on the domain (x,y).

Each of these three manners to represent a function has specific characteristics that complement one another. In this section we take a brief look at implicit representations of functions, curves and surfaces, mainly from the perspective of first-order approximations and, in particular, the respective gradient.

Let us start with on of the simplest possible restrictions in $\mathbb{R}^2$:

$$x - 3 = 0 \tag{48}$$

corresponding to the vertical line $x = 3$, passing through the point $(3,0)$, leaving the other coordinate y unconstrained. In $\mathbb{R}^3$, this same restriction would imply a vertical plane parallel to the $y \times z$ plane. In case we wanted a line in $\mathbb{R}^3$, we would need an additional restriction, e.g.:

$$y - 3 = 0. \tag{49}$$
$$x - 2 = 0 \tag{50}$$

which would therefore define a vertical line parallel to z, passing through $(3,2,0)$. Observe that if we impose one restriction to a space with dimension N, a mathematical structure with dimension $N-1$ will result. In case R non-redundant restrictions are considered, the structure will have at most $N - R$ dimensions. Observe that, for example, two restrictions defining two parallel, but not identical, planes in $\mathbb{R}^3$ will still imply a $2D$ structure.

The straight line for finite slope m can be defined as a single variable function:

$$y = m\,x + c \tag{51}$$

It immediately follows that:

$$g(x,y) = y - m\,x - c = 0 \tag{52}$$

which can also represent lines with infinite slope, as is the case of our previous example above, because no mapping as a graph is involved.

The circle with radius ρ centered at (x_c, y_c) can be implicitly represented as:

$$g(x,y) = \sqrt{(x-x_c)^2 + (y-y_c)^2} - \rho = 0 \tag{53}$$

Let us try to transform this equation into a graph form in the case $(x_0, y_0) = (0,0)$ and $\rho = 1$:

$$\sqrt{x^2 + y^2} = 1 \Longrightarrow$$
$$x^2 + y^2 = 1 \Longrightarrow$$
$$y = \sqrt{1 - x^2}$$

We have two possible solutions:

$$y_1 = +\sqrt{1 - x^2} \tag{54}$$
$$y_2 = -\sqrt{1 - x^2} \tag{55}$$

Each of then corresponds to a distinct graph representation of one of two halves of a circle. It follows that implicit functions can lead to more than one graph representation, involving possible decisions to be taken, as in the previous example.

As a more intricate example, let us consider the *Cassini oval* which, in implicit form, can be written as:

$$\sqrt{(x^2 + y^2)^2 - a(x^2 - y^2)} = 0 \tag{56}$$

with $a \in \mathbb{R}$.

Cassini ovals are interesting closed curves obtained in a manner analogous to an ellipse, but considering constant product, instead of sum, of distances to the two considered foci. Figure 12(a) illustrates a set of Cassini ovals obtained by varying the level set values.

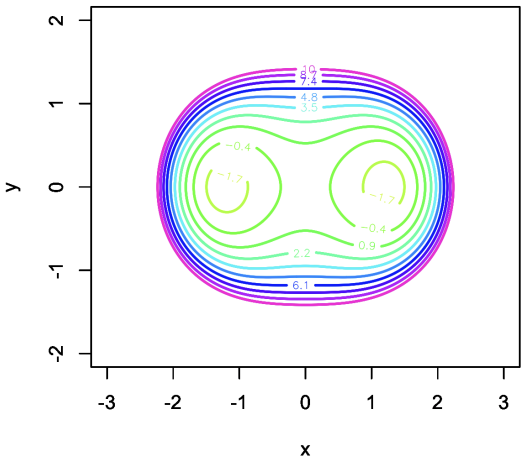

Figure 12: Cassini ovals obtained by varying the level set values from -3 to 10.

Though it is immediate to transform a graph form of a curve into a respective implicit representation, the opposite can be challenging or even impossible. As an example of the latter situation, we have the implicit function:

$$c\,\sin(x\,y) = x\,y$$

where c is a non-zero real-valued constant.

The *implicit function theorem* (e.g. []) provides the conditions in which an implicitly represented function can be solved in terms of the coordinates x, y and z, but even so the explicit representation may not be possibly obtained.

For a function $g(x, y) = 0$ in $2D$, provided that:

$$\frac{\partial g}{\partial y}\Big|_{(x_c, y_c)} \neq 0 \tag{57}$$

this theorem states provides a sufficient condition for expressing this curve as an explicit function $y = h(x)$ around a neighborhood of (x_0, y_0). Observe that this condition is simply verifying wether the function $y = y(x)$ takes infinite slope in the considered neighborhood, in which case it cannot be represented as a graph function. In higher dimensional cases, this theorem takes into account wether the respective Jacobian (a matrix of first-order derivatives) is invertible or not.

Given a $2D$ function in implicit form $g(x, y) = 0$, its first derivative can be calculated as:

$$\dot{g}(x) = -\frac{\frac{\partial g}{\partial x}}{\frac{\partial g}{\partial y}} \tag{58}$$

As an example, let us calculate the first derivative of the function in Equation 52:

$$\frac{\partial g}{\partial x} = -m; \quad \frac{\partial g}{\partial y} = 1$$

and we get:

$$\dot{g}(x) = -\frac{-m}{1} = m$$

which does correspond to the first derivative of the function $g(x, y)$ at each of its points (x, y). This property provides an effective manner for obtaining the derivative of $2D$ curves, to be used in respective first-order approximations.

As with curves, surfaces can also be defined in implicit manner. We have already seem that $x - 3 = 0$ defines a plane in $\mathbb{R}^3$. Let us consider some further examples:

A generic plane in $\mathbb{R}^3$ can be represented implicity as:

$$g(x, y, z) = a\,x + b\,y + c\,z + d = 0 \tag{59}$$

The sphere with radius ρ centered at (x_c, y_c, z_c) can be implicitly represented as:

$$\tilde{g}(x, y, z) = \sqrt{(x - x_c)^2 + (y - y_c)^2 + (z - z_c)^2} - \rho = 0 \tag{60}$$

The same surface can also be expressed as:

$$g(x, y, z) = (x - x_c)^2 + (y - y_c)^2 + (z - z_c)^2 \pm \rho^2 = 0 \tag{61}$$

One particularly interesting property of implicit representation of surfaces is that the respective *normal field* can be obtained simply as being parallel to the respective $3D$ gradient:

$$\boldsymbol{\nabla} g(x, y, z) \tag{62}$$

As an example, let us obtain a normal field $\boldsymbol{b}$ to the sphere in the above example:

$$\begin{aligned}
\frac{\partial g}{\partial x} &= 2(x - x_c) \\
\frac{\partial g}{\partial y} &= 2(y - y_c) \\
\frac{\partial g}{\partial z} &= 2(z - z_c) \\
\boldsymbol{n} = \boldsymbol{\nabla} g\big|_{(x_0, y_0)} &= \frac{\partial g}{\partial x}\hat{i} + \frac{\partial g}{\partial x}\hat{j} + \frac{\partial g}{\partial x}\hat{k}
\end{aligned} \tag{63}$$

Observe that the obtained results do not depend on ρ, indicating that the gradient is actually "seeing" the homogeneous scalar field $\tilde{g}(x, y, z) = (x - x_c)^2 + (y - y_c)^2 + (z - z_c)^2$, of which the above sphere is but a level set. As a consequence, the gradient will correspond, in the $3D$ space, to the *normal* to the sphere in Equation 61 specified by a particular value of ρ.

Figure 13 illustrates the projection onto the (x, y) plane of the above obtained gradient considering $z = 1$, $(x_c, y_c, z_c) = (2, 2, 1)$ and $\rho = 2$. It can be immediately observed that this gradient provides a vector field that is normal to the original surface.

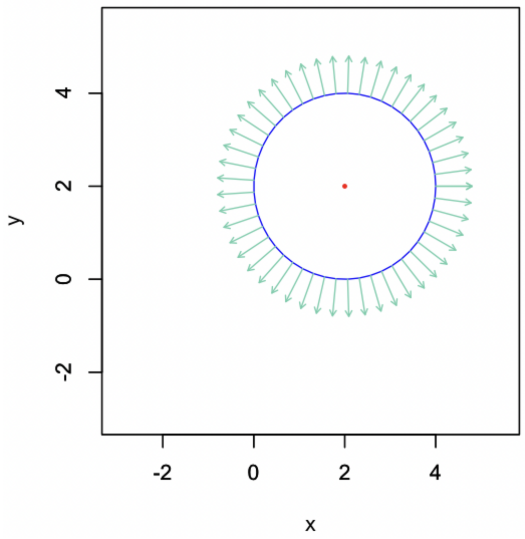

Figure 13: A normal field obtained for a sphere with $(x_c, y_c, z_c) = (2, 2, 1)$ and $\rho = 2$ sliced at $z = 1$ and projected onto the (x, y) plane. The projected gradient is shown to 50% scale for the sake of enhanced visualization.

It is interesting to observe that the implicit representation of the sphere allowed a respective normal field to be obtained in a particularly straightforward manner.

As an additional example, let us derive the implicit representation of a paraboloid in 3D, and calculate the respective normal field.

We start by writing the graph representation of the paraboloid centered at (x_c, y_c) as a function of (x, y):

$$\begin{aligned} r &= \sqrt{(x-x_c)^2 + (y-y_c)^2} \\ z &= r^2 = (x-x_c)^2 + (y-y_c)^2 \end{aligned} \tag{64}$$

so that a respective implicit representation is as follows:

$$(x-x_c)^2 + (y-y_c)^2 - z = 0 \tag{65}$$

The respective gradient is:

$$\begin{aligned} \frac{\partial g}{\partial x} &= 2(x-x_c) \\ \frac{\partial g}{\partial y} &= 2(y-y_c) \\ \frac{\partial g}{\partial z} &= -1 \\ \boldsymbol{n} = \boldsymbol{\nabla} g\big|_{(x_c,y_c)} &= \frac{\partial g}{\partial x}\hat{i} + \frac{\partial g}{\partial x}\hat{j} + \frac{\partial g}{\partial x}\hat{k} \end{aligned} \tag{66}$$

The projection onto the (x, y) plane of the above gradient considering obtained for the paraboloid with $(x_c, y_c, z_c) = (2, 2, 1)$, sliced at $z = 1$, is depicted in Figure 14.

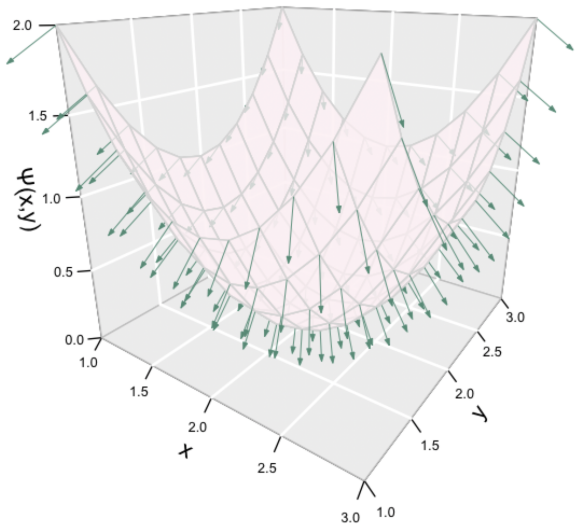

Figure 14: The normal field of a paraboloid with $(x_c, y_c) = (2, 2)$. The gradient is shown to 20% scale for the sake of enhanced visualization.

It should be kept in mind that projections of the obtained $3D$ gradient onto the (x, y) plane will *not* necessarily correspond to the gradient of the respective graph representation. Even though these two vector fields will be mutually parallel, one of them may have opposite direction than the other (recall that two opposite vectors are also parallel one another). This is a consequence of the fact that both $g(x, y, z)$ and $-g(x, y, z)$, having oppositely oriented gradients, will correspond to the same original surface.

7 Graph Surfaces and Local Frames

In Section 2, we approached the interesting task of assigning a local frame that adapted to a given function around a small neighborhood of a reference point x_0. This problem was addressed in a more comprehensive manner in Section 4, respectively to parametric curves. In both cases, we were able to define, from first-order approximations of the original function/curve, reference frames that were independent of the adopted coordinate system.

In this section, we develop an approach to obtaining local reference frames for multivariate functions and graph surfaces that do not depend on the specific choice of orthonormal coordinate system.

Our objective here is to define an orthogonal frame at a chosen reference point (x_0, y_0) that adapts locally to the curve shape around that point. In the case of single-variable functions and parametric curves, we resourced to the tangent as a reference for adapting our system. In the case of multivariate functions and surfaces, however, more than one tangent can be defined along the surface at the reference point.

An interesting possibility to follow in this case consists of considering the normal field to the surface, from which the plane that is tangent to that same surface can be readily determined. Then, we are left with the task of orienting a respective set of orthogonal vectors onto this plane, therefore defined a possible reference frame.

We will illustrate this approach, as described in the following, respectively to a specific multivariate paraboloid given as:

$$\begin{aligned} &z = f(x,y) = -(x-x_c)^2 - (y-y_c)^2 \quad \text{(graph repr.)}; \\ &-z - (x-x_c)^2 - (y-y_c)^2 = 0 \quad \text{(implicit repr.)} \end{aligned}$$

with $(x_c, y_c) = (2, 3)$.

We obtain the $3D$ gradient of the respective implicit representation as follows:

$$\begin{aligned} \frac{\partial g}{\partial x} &= -2(x-2) \\ \frac{\partial g}{\partial y} &= -2(y-3) \\ \frac{\partial g}{\partial z} &= -1 \\ \boldsymbol{n} = \boldsymbol{\nabla} g\big|_{(x_c,y_c)} &= \frac{\partial g}{\partial x}\hat{i} + \frac{\partial g}{\partial x}\hat{j} + \frac{\partial g}{\partial x}\hat{k} \end{aligned} \tag{67}$$

Let us consider $(x_0, y_0) = (2, 2)$ as the reference point, which implies:

$$\boldsymbol{n} = 0\,\hat{i} + 2\,\hat{j} - 1\,\hat{k} \tag{68}$$

However, we shall take the inverse of the above vector, so that the normal points outward from the paraboloid surface:

$$\boldsymbol{n} = 0\,\hat{i} - 2\,\hat{j} + 1\,\hat{k} \tag{69}$$

As it turned out, the determination of the normal field was straightforward for this considered surface, illustrating the effectiveness of the implicit representation approach.

Now, we need to find two orthogonal vectors $\boldsymbol{t}$ and $\boldsymbol{b}$ belonging to the plane perpendicular to the normal field at the reference point (x_0, y_0). Actually, we only need to determine one of them, as the other can be obtained by the cross-product of the former two vectors. Observe that any vector belonging to the perpendicular plane will be automatically tangent to the surface at (x_0, y_0).

One particularly interesting possibility is to find a reference frame that does not depend on rotations or translations of the coordinate system, and that also reflects the local shape of the surface around the reference point. We already have a normal vector that has these two properties, though its direction may have been determined while taking into account the $z-$axis direction.

In this sense, one particularly interesting possibility is to consider the tangent vector that coincides with the tangent of a $3D$ parametric curve contained (embedded) in the original surface which has the largest curvature at (x_0, y_0).

Let us approach this problem by considering the embedded curves to be defined by all possible intersections between the paraboloid and planes that are orthogonal to the (x, y) plane and pass through $(x_0, y_0) = (2, 2)$, which imply in the following generic parametric straight curves on the (x, y) plane:

$$\begin{cases} x(t) = [\cos(\theta)\, t + 2] \\ y(t) = [\sin(\theta)\, t + 2] \end{cases} \tag{70}$$

Recall that the peak of the paraboloid is centered at $(x_c, y_c) = (2, 3)$. By substituting the above expressions in the paraboloid graph equations, it follows that:

$$z = -\,(x-2)^2 - (y-3)^2\,;$$
$$z = f(t) = -\,[\cos(\theta)\, t]^2 - [\sin(\theta)\, t - 1]^2$$

The respective derivatives are:

$$\dot{f}(t) = -2t\cos^2(\theta) - 2\,\sin(\theta)\,[\sin(\theta)\, t - 1]\,;$$
$$\ddot{f}(t) = -2\cos^2(\theta) - 2\sin^2(\theta) = -2$$

The curvature of any of the above single-variable functions $z = f(t)$ can now be calculated as:

$$\kappa(t) = \frac{\left|\ddot{f}(t)\right|}{\left(1 + \dot{f}^2(t)\right)^{3/2}}$$

At $t = 0$, which specifies point (x_0, y_0), we have:

$$\kappa(t=0) = \frac{|-2|}{\left(1 + 4\,\sin^2(\theta)\right)^{3/2}} = \frac{2}{\left(1 + 4\,\sin^2(\theta)\right)^{3/2}}$$

which is maximized when $\sin(\theta) = 0 \Rightarrow \theta = 0$, with the maximum curvature being equal to:

$$\kappa(t) = \frac{2}{\left(1 + 4\,\sin^2(0)\right)^{3/2}} = 2$$

As an aside, the *maximum* curvature is known as the *first principal curvature* κ_1 of the surface at a specific reference pointe. The *second principal curvature* κ_2 is defined as corresponding to the *minimal* curvature at the same reference point. These two curvatures are said to be *extrinsic*, as they depend on how the surface is embedded into a given space. A simple example of extrinsic property is the angle of a tangent with respect to any of the axes, which changes as the basis is rotated. In contrast, *intrinsic* properties of the surface (or curve) do not depend on the embedding. An example of intrinsic property is the product $\kappa_1\,\kappa_2$, which is called *Gaussian curvature*, while the mean between κ_1 and κ_2 is said to be the *mean curvature*.

Going back to our Frenet trihedron, given that $\theta = 0$, we can choose the orientation along the $x-$axis, which we take as having the same orientation and direction than x. Thus, we obtain the following tangent vector:

$$\boldsymbol{t} = 1\,\hat{\boldsymbol{i}} + 0\,\hat{\boldsymbol{j}} + z_t\,\hat{\boldsymbol{k}}$$

in order to determine z_t, we consider that it is perpendicular to the normal vector, hence:

$$\boldsymbol{t} \cdot \boldsymbol{n} = (1, 0, z_t) \cdot (0, -2, 1) = 0 \Longrightarrow$$
$$\Longrightarrow 0 + z_t = 0 \Longrightarrow z_t = 0$$

and we obtain:

$$\boldsymbol{t} = 0\,\hat{\boldsymbol{i}} - 1\,\hat{\boldsymbol{j}} + 0\,\hat{\boldsymbol{k}}$$

The third vector needed to complete our orthogonal basis can be now determined as:

$$\boldsymbol{b} = \boldsymbol{t} \times \boldsymbol{n} = 0\,\hat{\boldsymbol{i}} - 1\,\hat{\boldsymbol{j}} - 2\,\hat{\boldsymbol{k}}$$

which therefore is biorthogonal to the other two previous vectors, defining a right-hand basis.

An orthogonal basis $(\boldsymbol{t}, \boldsymbol{n}, \boldsymbol{\tau})$ reflecting locally the first-order shape of the surface is therefore given as follows:

$$\begin{cases} \boldsymbol{t} = 1\,\hat{\boldsymbol{i}} + 0\hat{\boldsymbol{j}} + 0\hat{\boldsymbol{k}};. \\ \boldsymbol{n} = 0\,\hat{\boldsymbol{i}} - 2\hat{\boldsymbol{j}} + 1\,\hat{\boldsymbol{k}}; \\ \boldsymbol{\tau} = 0\,\hat{\boldsymbol{i}} - 1\,\hat{\boldsymbol{j}} - 2\,\hat{\boldsymbol{k}} \end{cases}$$

In summary, at (x_0, y_0) we have that $\boldsymbol{n}$ indicates the normal to the surface, $\boldsymbol{t}$ has the orientation leading to the maximum surface curvature at (x_0, y_0), and $\boldsymbol{b}$ is directly determined from the two former vectors, so that the three vectors are mutually orthogonal while defining a right-hand system of coordinates.

Except for decisions regarding the orientation of the normal and tangent vectors, the obtained frame is independent of the choice among orthonormal coordinate systems, while reflecting closely the first-order shape of the surface (observe that we did not resource to any second or higher order derivatives of the surface) around a small neighborhood of the reference point (x_0, y_0). If needed, this orthogonal frame can be readily normalized so as to become orthonormal.

A first-order local coordinate system can now be obtained by translating the old orthogonal system, here understood to be the Euclidean space $\mathbb{R}^3$, to the reference point (x_0, y_0, z_0) and then implementing the transformation to the new basis $(\boldsymbol{t}, \boldsymbol{n}, \boldsymbol{b})$. Figure 15 illustrates the so-obtained new coordinate system.

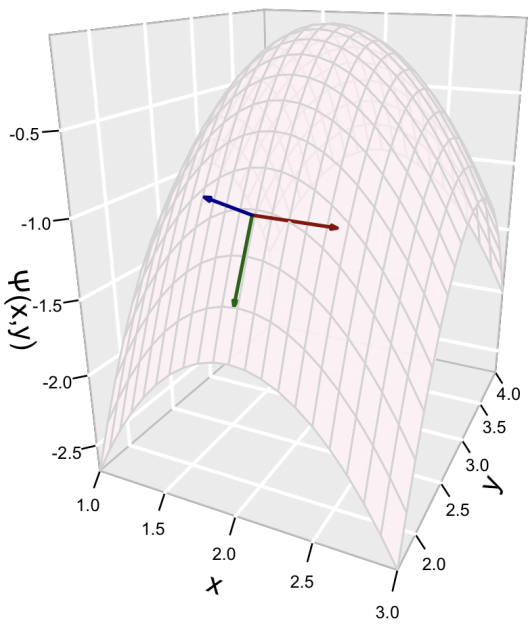

Figure 15: The Frenet trihedron obtained for the paraboloid. Observe how this frame adapts to the surface, with the tangent (red) and binormal (green) vectors being contained in the respective tangent plane, while being orthogonal to the normal vector (in blue). The vectors, shown after being normalized for unit magnitude, have been scaled down by 50% for the sake of enhanced vizualization.

8 Approximating Vector Fields

Thus far, in the present work, the generality of first-order approximations has been illustrated respectively to several mathematical entities, including single and multiple-variable functions, curves, and surfaces.

It turns out that first-order can also be considered as a means to approximate *vector fields*, in which vectors from a space S are transformed into another space $\tilde{S}$. These vector fields can be understood either as mappings between vectors, or transformations of the original space into a new, possibly non-linear space.

The key concept underlying first-order approximations of vector fields consists in the Jacobian of the *vector field*, which plays a role analogous to the gradient in multivariate functions, and to the first derivative in single-variable functions. The Jacobian of a vector field $\boldsymbol{\phi}(\phi_x(x,y,z), \phi_y(x,y,z), \phi_z(x,y,z))$ can be expressed as follows:

$$J = \begin{bmatrix} \frac{\partial\,\phi_x}{\partial x} & \frac{\partial\,\phi_x}{\partial y} & \frac{\partial\,\phi_x}{\partial z} \\ \frac{\partial\,\phi_y}{\partial x} & \frac{\partial\,\phi_y}{\partial y} & \frac{\partial\,\phi_y}{\partial z} \\ \frac{\partial\,\phi_z}{\partial x} & \frac{\partial\,\phi_z}{\partial y} & \frac{\partial\,\phi_z}{\partial z} \end{bmatrix} \tag{71}$$

Now, given differential displacements dx, dy, and dz along each of the respective axes, the differential variation of the vector field, which is itself a $3D$ vector, can be quantified as the following set of three "parallel" total derivatives:

$$\boldsymbol{d\,\phi} = \begin{bmatrix} d\,\phi_x \\ d\,\phi_y \\ d\,\phi_z \end{bmatrix} = \begin{bmatrix} \frac{\partial\,\phi_x}{\partial x} & \frac{\partial\,\phi_x}{\partial y} & \frac{\partial\,\phi_x}{\partial z} \\ \frac{\partial\,\phi_y}{\partial x} & \frac{\partial\,\phi_y}{\partial y} & \frac{\partial\,\phi_y}{\partial z} \\ \frac{\partial\,\phi_z}{\partial x} & \frac{\partial\,\phi_z}{\partial y} & \frac{\partial\,\phi_z}{\partial z} \end{bmatrix} \begin{bmatrix} dx \\ dy \\ dz \end{bmatrix} \tag{72}$$

In the particular case in which $\boldsymbol{\phi}()$ is a linear map specified by a respective matrix A, we have that $J = A$. For instance, in the case of the above example for the sheared coordinate change, we have:

$$\begin{bmatrix} \tilde{x} \\ \tilde{y} \end{bmatrix} = \begin{bmatrix} 1 & 2 \\ -1 & 1 \end{bmatrix} \begin{bmatrix} x \\ y \end{bmatrix} \tag{73}$$

The fact that this mapping can be understood as a vector field can be better appreciated by rewriting the equation above as:

$$\begin{aligned} \phi(x,y) = (\phi_x(x,y), \phi_y(x,y)) \Longrightarrow \\ \Longrightarrow \begin{cases} \phi_x(x,y) = \tilde{x} = \tilde{x} + 2\,\tilde{y} \\ \phi_y(x,y) = \tilde{y} = -\tilde{x} + \tilde{y} \end{cases} \end{aligned} \tag{74}$$

Therefore:

$$\frac{\partial \phi_x}{\partial x} = 1; \qquad \frac{\partial \phi_x}{\partial y} = 2$$
$$\frac{\partial \phi_y}{\partial x} = -1; \qquad \frac{\partial \phi_y}{\partial y} = 1$$

So that the Jacobian of the vector field associated to this transformation corresponds to direct transformation matrix A, i.e.:

$$J = \begin{bmatrix} 1 & 2 \\ -1 & 1 \end{bmatrix} = A \tag{75}$$

A particularly important property of the Jacobian is that it provides the *best linear approximation* of the map $\boldsymbol{\phi}()$ around each point $\boldsymbol{v}_0 = (x_0, y_0, z_0)$ of the considered space as follows:

$$\boxed{\tilde{\boldsymbol{\phi}}(\boldsymbol{v})\big|_{\boldsymbol{v}_0} \approx \boldsymbol{\phi}(\boldsymbol{v}_0) + J(\boldsymbol{v}_0)\,(\boldsymbol{v} - \boldsymbol{v}_0)} \tag{76}$$

where $\boldsymbol{v}$ is a generic vector.

A direct analogy can be observed between the above expression and the Taylor series in Equation 2. Indeed, the Jacobian is understood as the first-order differential of the vector field $\boldsymbol{\phi}()$, in direct analogy to the tangent, which is the first-order differential of single-variable functions.

The above approximation can be particularly effective as a means to study and handle non-linear vector fields. Similarly to the concepts and possibilities discussed in Section 2, the idea is to perform one or more approximations of the non-linear vector field around a specific point of interest $\boldsymbol{v}_0 = (x_0, y_0, z_0)$.

Figure 16 illustrates the first-order approximation of the vector field:

$$\begin{cases} \phi_x(x, y) = x^2\, y \\ \phi_x(x, y) = x\, y \end{cases} \tag{77}$$

around the reference point $(x_0, y_0) = (0.35, 0.52)$ obtained by the Taylor series, in terms of the respective Jacobian.

In addition to the effectiveness of the Jacobian to provide for linear approximations, its *determinant* $det(J)$, called *Jacobian determinant*, can provide important information about the local properties of the map around the reference vector $\boldsymbol{v}_0$, including:

- $|det(J)|$ indicates how the hypervolume changes around each point, expanding for $|det(J)| > 1$ and shrinking for $0 < |det(J)| < 1$;
- $det(J) > 0$ means that the direction of the vectors is maintained around each point;
- $det(J) < 0$ means that the direction of the vectors is reversed around each point;
- the map is invertible around each point iff $det(J) \neq 0$.

Let us illustrate the potential of the Jacobian respectively to two situations: (a) the two sheared transformations discussed in Section 2; and (b) a non-linear vector field.

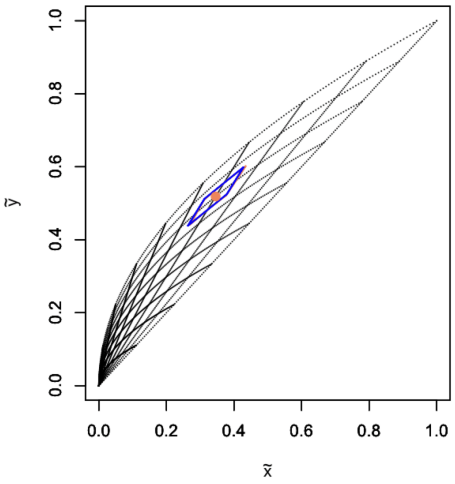

(a)

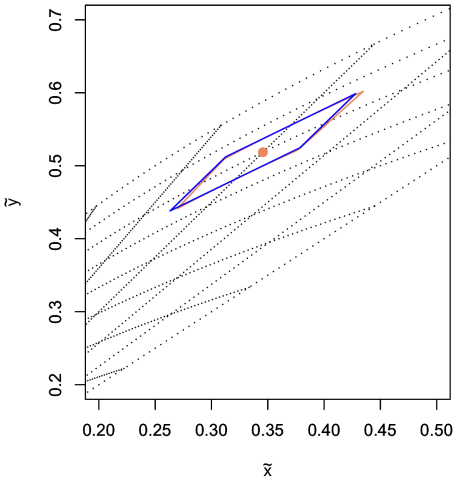

(b)

Figure 16: (a): The first-order approximation of the vector field in Eq. 77 around the reference point $(x_0, y_0) = (0.35, 0.52)$ (shown in red). The mapping of the boundary of a small neighborhood around this reference point has also been shown in this figure, yielding markedly similar results between the non-linear mapping (in red) and first-order approximation (in blue). The sheared mesh, shown as dotted curves, corresponds to the mapping by the original non-linear vector field of a regular reticulate in the original space. (b) Zooming into the mapping in (a).

Observe that, given that the Jacobian matrix of a linear transformation is constant (i.e. does not depend on x or y), the indications provided by the Jacobian determinant apply to every generic point (x, y). In the more general case of non-linear transformations, the indications provided by the Jacobian and its determinant apply only around a small neighborhood around a point of reference $\boldsymbol{v}_0$.

We start with the orthonormal transformation implied

by the matrix:

$$A = \begin{bmatrix} \frac{\sqrt{2}}{2} & -\frac{\sqrt{2}}{2} \\ \frac{\sqrt{2}}{2} & \frac{\sqrt{2}}{2} \end{bmatrix} \tag{78}$$

Its determinant is $\det(A) = 1$, because it is an orthonormal matrix, meaning that there will be no changes of magnitudes and that the geometry will be fully preserved up to a rotation.

Let us now consider the matrix:

$$A = \begin{bmatrix} 1 & 2 \\ -1 & 1 \end{bmatrix} \tag{79}$$

Its determinant is $\det(A) = 3$, indicating that volume expansion and preservation of vector directions.

Now, consider the following non-linear vector field:

$$\boldsymbol{\phi}(x, y) = \begin{cases} \phi_x(x, y) = xy \\ \phi_y(x, y) = x^2 \end{cases} \tag{80}$$

The respective Jacobian is given as:

$$J = \begin{bmatrix} y & x \\ 2x & 0 \end{bmatrix}$$

The respective determinant corresponds to the following scalar field:

$$det(J) = -2x^2$$

Figure 17 depicts the determinant of the vector field $\boldsymbol{\phi}(x, y)$ for $x \in [-2, 2]$ and $y \in [-2, 2]$.

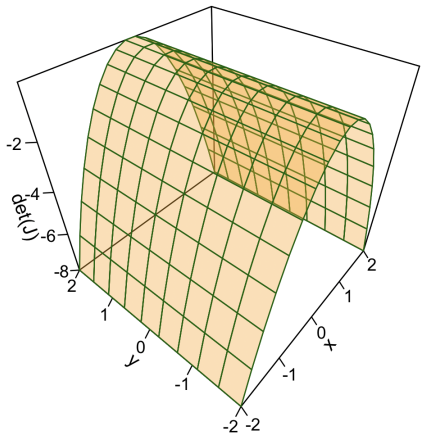

Figure 17: The values of the determinant of the Jacobian of the vector field in Eq. 80, considering $x \in [-2, 2]$ and $y \in [-2, 2]$, provide an objective quantification of the local expansion/contraction implemented by the map, the preservation (or not) of vector direcdtion, as well as local differentiability. In this case, contraction and direction inversion will be implemented by the respective vector field mapping.

9 First-Order Approximation Error

Before concluding the present work, it is interesting to pay at least some brief attention to the accuracy allowed by first-order approximations.

One first important aspect to be realized is that the first-order approximation accuracy depends on two main factors: (i) the type and properties of the specific function being approximated; and (ii) the points around which the approximations are considered.

In the case of single-variable functions, it can be shown that the first-order approximation:

$$g(x) \approx y(x) = y(x_0) + \dot{g}(x_0)\,(x - x_0)$$

incurs an error given as:

$$\varepsilon(v) = \ddot{g}(v)\,(x - x_0)$$

for some value v comprised in the interval $[x_0, x]$, so that we can write:

$$g(x) = y(x_0) + \dot{g}(x_0)\,(x - x_0) + \varepsilon(v)$$

This results confirms that the error depends on the specific function $g(x)$, as well as the specific neighborhood considered in the approximation.

As an illustration, let us consider the possible error while of the first order approximation of the functions:

$$g_2(x) = x^2$$
$$g_3(x) = x^3$$

we immediately have that:

$$\varepsilon_2(v) = 2v\,(x - x_0)$$
$$\varepsilon_3(v) = 3v^2\,(x - x_0)$$

In case we are interested in approximations in the interval $0 \leq x \leq 1$ (considering $x_0 = 0$), we would have the respective error as illustrated in Figure 18. As expected, we have that the error depends on the interval, and also on the type of function.

Indeed, the errors obtained for the third-degree function $g_3(x) = x^3$ are larger, but not substantially so, when compared to the errors for $g_2(x) = x^2$. At the same time, the error increases more markedly with x in the case of the higher-degree polynomial. In other words, higher degree polynomials will imply potentially larger first-order approximation errors.

The error when approximating non-polynomial functions can be estimated in a similar manner as discussed above.

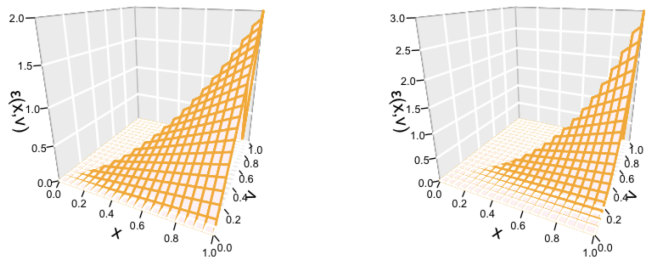

(a) (b)

Figure 18: The maximum error that can be incurred in the approximation of the single-variable functions $g(x) = x^2$ (a) and $g(x) = x^2$ (b) in terms of $x \in [0, 1]$ and $v \in [0, x]$.

10 Concluding Remarks

Science and technology have undergone remarkable progress while relying intense and extensively on mathematical concepts and methods, of which integro-differential calculus has been particularly important. Being a related topic, first-order approximations underliy an ample range of theoretical and applied approaches. However, perhaps as a consequence of being so frequently used, the special role that first order approximations have seems sometimes to go unnoticed.

The present work was aimed at providing a (hopefully) accessible introduction to first-order approximations relatively to several types of mathematical structures, including single- and multi-variable functions, curves, and surfaces, as well as vector fields. Several numerical examples and illustrations have been incorporated in order to contribute with the familiarization with the respective concepts and methods.

In particular, we have seen how general, versatile and powerful first-order approximations can be regarding most related operations, including extrapolation, integration, and identification of particularly interesting basis and coordinate systems that effectively adapt to the local shape of functions, curves, surfaces, and vector fields.

As observed in the introduction, despite their widespread application and effectiveness, first-order approximations cannot comprehensively represent non-linear systems along larger regions. Additional concepts and methods, including second and higher-order approximations in the respective Taylor series are required, which deserve further attention. It is hoped that the present work may motivate and facilitate such subsequent studies.

Acknowledgments

Luciano da F. Costa thanks CNPq (grant no. 307085/2018-0) and FAPESP (grant 15/22308-2).

Observations

As all other preprints by the author, the present work contains preliminary work subject to further revision and validation. Respective modification, commercial use, or distribution of any of its parts are not possible, as this work has author copyright. Many of the preprints by the author are also available in Hal and/or arXiv. This work can also be cited by using the DOI number or article identification link. Thanks for reading.

References

[1] L. da F. Costa. Visual saliency and attention as random walks on complex networks. arXiv, 2006. https://arxiv.org/abs/physics/0603025.

[2] L. da F. Costa. *Shape Classification and Analysis: Theory and Practice*. CRC Press, Boca Raton, 2nd edition, 2009.

[3] L. da F. Costa. A journey into the multifaceted universe of coordinates change, basis transformation, dual spaces, and invariance. Researchgate, 2020. https://www.researchgate.net/publication/366840988_A_Journey_into_the_Multifaceted_Universe_of_Coordinates_Change_Basis_Transformation_Dual_Spaces_and_Invariance.

[4] J. H. Hubbard and B. B Hubbard. *Vector Calculus, Linear Algebra, and Differential Forms: A Unified Approach*. Prentice Hall, 2001.

[5] K. Hoffman. *Linear Algebra*. Pearson India, 2015.

[6] R. Larson, R. P. Hostetler, B. H. Edwards, and D. E. Heyd. *Calculus with analytic geometry*. DC Heath Lexington, Massachusetts, USA, 1986.

[7] T. M. Apostol. *Calculus*. Wiley and Sons, 2019.

[8] L. da F. Costa. A mosaic of multivariate calculus. Researchgate, 2020. https://www.researchgate.net/publication/340570370_A_Mosaic_of_Multivariate_Calculus_CDT-27.

[9] C. H. Edwards and D. E. Penney. Calculus with geometry analytic, 2002.

[10] L. da F. Costa. Point motion in flat spaces: An ample starting point. https://www.researchgate.net/publication/365806206_Point_Motion_in_Flat_Spaces_An_Ample_Starting_Point, 2022.